
HYPERPARAMETER-FREE DEEP ACTIVE LEARNING FOR REGRESSION PROBLEMS VIA QUERY SYNTHESIS

A PREPRINT

Simiao Ren, Yang Deng, Willie J. Padilla and Jordan M. Malof

Department of Electrical and Computer Engineering

Duke University

Durham, NC 27705, USA

jordan.malof@duke.edu

ABSTRACT

In the past decade, deep active learning (DAL) has heavily focused upon classification problems, or problems that have some ‘valid’ data manifolds, such as natural languages or images. As a result, existing DAL methods are not applicable to a wide variety of important problems – such as many scientific computing problems – that involve regression on relatively unstructured input spaces. In this work we propose the first DAL query-synthesis approach for regression problems. We frame query synthesis as an inverse problem and use the recently-proposed neural-adjoint (NA) solver to efficiently find points in the continuous input domain that optimize the query-by-committee (QBC) criterion. Crucially, the resulting NA-QBC approach removes the one sensitive hyperparameter of the classical QBC active learning approach - the “pool size” - making NA-QBC effectively hyperparameter free. This is significant because DAL methods can be detrimental, even compared to random sampling, if the wrong hyperparameters are chosen. We evaluate Random, QBC and NA-QBC sampling strategies on four regression problems, including two contemporary scientific computing problems. We find that NA-QBC achieves better average performance than random sampling on every benchmark problem, while QBC can be detrimental if the wrong hyperparameters are chosen.

Keywords Deep Learning · Active Learning · Regression · Query-by-committee · Query Synthesis · Inverse Problem · Scientific Computing · Artificial Electromagnetic Material

1 Introduction

Deep learning has led to major advances in many areas of science and engineering [1, 2, 3], however one of its major limitations is the need for large quantities of labeled data. One widely-studied method to reduce the data needs of machine learning models is active learning (AL) [4, 5, 6]. In AL it is assumed that data can vary in its “informativeness” for training, and that the required quantity of labeled training data (e.g., to reach some level of model accuracy) can be reduced by choosing the most informative data to label, or *query*, and include in the training dataset [5]. Therefore the learning algorithm (the learner) not only learns to fit the data, but also to choose the data from which it learns (e.g., it designates unlabeled data to label for inclusion in the training dataset).

There are three well-known AL paradigms [4, 5, 6]: (a) pool-based (b) stream-based (c) and query synthesis (QS). In the first two paradigms the learner must choose the best instance to label from among a finite and pre-defined set of candidates. By contrast, in QS the learner can query any point(s) from within the input data domain. In principle therefore QS can find superior query points because it has a much larger (sometimes infinite) set of candidates to choose from. However, searching over these large input spaces can be slow, especially if the learner is a large model such as a deep neural network (DNN); the learner is typically utilized in the computation of informativeness (e.g., in entropy-based or QBC-based measures [7]).

In recent years several active learning methods have been developed specifically for DNNs - sometimes called deep active learning methods [8] - but the majority of these approaches have focused upon the pool-based AL paradigm

[4]. A few methods have been proposed QS as well [9, 10, 11], however these methods are designed specifically for classification problems, excluding their use in other important tasks such as regression. As a result, these QS methods exclude many important application areas in science and engineering that are increasingly impacted by deep learning. This includes emerging applications of DNNs in chemistry [12], materials science [13], and biology [14] where DNNs are used to model the behavior and properties of various systems. In this work our experiments will consider two contemporary problems in materials science where DNNs have recently been used to predict the properties of materials - both regression problems.

1.1 Contribution of this work

In this work we propose the first DNN-based QS approach for regression problems. Our approach relies upon the widely-known query-by-committee (QBC) criteria, which is computationally intensive for DNNs because it involves evaluating several DNNs for each candidate query point. This can be made more efficient by using Dropout as done in [15], however it is still costly to search point-wise over large or continuous input spaces. To overcome this problem, we frame AL as an inverse problem where our goal is to find input values that maximizes the QBC criterion, and then employ the recently-proposed neural-adjoint (NA) approach to efficiently solve the optimization problem using gradient-based search.

Importantly, the resulting NA-QBC approach removes the primary sensitive hyperparameter of QBC - its "pool size". The pool size hyperparameter determines how many candidate query points are evaluated in each iteration of AL. A larger pool size can lead to the discovery of more informative points because the input space is sampled more densely; however, larger pool sizes also tend to increase selection of redundant query points [16, 4, 17]. We discuss this limitation further in Section 3. Although it is rarely discussed in the literature, the effectiveness of QBC (and other pool-based AL methods) depends strongly upon the selection of an appropriate pool size, which varies widely across problems, and cannot easily be determined in advance (i.e., before labeling data). Therefore the dependency of QBC on pool size greatly undermines its practical utility because it is not clear whether it will, for example, outperform a naive random sampling strategy. While NA-QBC does have several hyperparameters, we say that it is "hyperparameter free" with respect to AL because its hyperparameters can be optimized in advance, without the availability of labeled training data.

To test these hypotheses we evaluate NA-QBC, QBC, and random sampling on four regression problems, including two contemporary regression problems from materials science. We show empirically that the performance of QBC varies strongly depending upon pool size, and that the best-performing pool size is problem-dependent. By contrast, we find that NA-QBC achieves performance comparable to that obtained by QBC when using its best pool size setting. Furthermore, we show that, when mimicking the hyperparameter selection scheme in real-life scenarios, NA-QBC almost always outperforms QBC. Furthermore, NA-QBC always provides advantages over random sampling, whereas QBC can sometimes perform worse than random sampling depending upon its pool size parameter. We now summarize the contributions of this work.

- **NA-QBC: the first query synthesis deep active learning model for regression.** This extends query synthesis active learning to many important problems in science and engineering that increasingly depend upon deep learning models.
- **We discuss and demonstrate the significance of hyperparameter selection for active learning models.** Although rarely discussed in the literature, pool-based AL methods are sensitive to the pool size hyperparameter. We discuss this limitation here and propose a measure of "real-world" AL performance. We use the proposed measure to evaluate the performance of QBC, as well as its sensitivity to its hyperparameters.
- **A zero hyperparameter version QBC approach, via query synthesis:** NA-QBC consistently outperforms random sampling, and does so without assuming knowledge of sensitive hyperparameters. This makes NA-QBC a much more reliable alternative to QBC.

The paper is organized as follows: Section 2 overviews related work. Section 3 discusses QBC and its hyperparameter problems, while Section 4 introduces the neural adjoint inverse solver and how its combination with QBC can mitigate the hyperparameter problem. Section 5 lays out the experiments and introduces the benchmark problems and section. Section 6 compares random sampling, QBC and NA-QBC.

2 Related works

Query synthesis active learning Although QS was proposed relatively early on [18], it has yet to make the same impact as pool-based methods, due to its difficulty to work together with human annotators [19]. Interpolation techniques between labeled data points were first investigated by [20] for the synthesized query. Following interpolation, [21]

proposed synthesizing the middle point of the closest opposite pair, which is restricted to classification problems. [22, 23] employed QS in real-life settings for automating biological experiments and achieved a much lower cost than humans. [24] derived the statistical optimal choice of a new query point that minimizes the variance of the learner but pointed out too many approximations were needed for neural networks to effectively use such techniques. [11] explored QS on one-class classifiers with evolutionary algorithms, non-trivial to convert to a regression setting. With deep learning, [9, 10, 25] used Generative Adversarial Networks (GAN) to synthesize new images for classification tasks, however transforming the GAN techniques into regression tasks is not intuitive due to the inherent "discriminator" portion of GAN. Although the GAN portion is hardly transferable to our problem setting, the gradient descent steps to search the space is close to NA-QBC in that both method use gradient information to guide the search for new query points.

The lack of attention for QS methods can also be seen in recent review papers, two recent reviews on active learning, while both acknowledging the existence of QS paradigm, did not discuss any specific QS algorithm [6, 4]. To our knowledge, only one review paper discussed QS [5] however, as it was published in the pre-ImageNet era, none of the QS strategies mentioned were based on deep learning.

Active learning for regression problems Although significant effort has pushed the boundary of active learning, only a few studies have focused on regression tasks. For example, in an ICML workshop on active learning and experimental design, the "Active Learning Challenge" [26] had all of their 6 benchmark datasets being binary classification tasks. For regression tasks, Expected model change [27] was explored, where an ensemble of models was used [28] to estimate the true label of new query point and Gaussian Process [29] were used with a natural estimate of variance on unlabeled points. [30] used QBC, which trains multiple networks and finds the most disagreeing unlabeled points of the committee of models trained. [15] used the Monte Carlo drop-out as an alternative to the QBC method to maximize the variance of committee members, which is now implicitly embedded in the dropout mechanism. Although these studies have investigated regression tasks, none of the above used QS paradigm.

3 Problem setting and query-by-committee

Let $T^i = (X^i, Y^i)$ be the dataset used to train one or more regression models at the i^{th} iteration of active learning, $i \in \mathbb{N}_0$. Since our focus is on deep active learning, we assume that the regression models of interest will be DNNs. We also assume that some relatively small number of N_{ini} randomly-sampled training instances are available to initially train the models, $T^0 = (X^0, Y^0)$. In our problem setting we assume that each query instance x must be sampled from some well-defined space of valid input values, χ , that can be easily sample (i.e., with little or no cost). This is a reasonable assumption in many problems in scientific computing for example, where the input parameters are defined by the scientist, or otherwise constrained by physical laws; this is the case for all of our benchmark problems. In each round of active learning, we are permitted to select K query instances $x_k \in \chi$ to be labeled by some oracle and added to the training dataset. Our goal is then to choose samples to maximize the performance of a DNN-based regression model at each iteration of active learning.

Query-by-Committee. Query-by-committee is a well-known pool-based active learning algorithm [7] where in each iteration of active learning we create a pool U of N_U input instances that are randomly sampled from χ . Then our goal is to choose the top k samples from U as determined by the following measure

$$\sigma_{QBC}^2 = \frac{1}{N} \sum_{n=1}^N (f_n(x) - \mathbb{E}_{n \in N} [f_n(x)])^2, x \in U \quad (1)$$

Here f_n denotes the n^{th} model in an ensemble of N_{ens} models. In each iteration of AL these models are trained on all available training data at that iteration. The measure in Eq. 1 is known as the QBC criterion and it is essentially the variance of the predictions of the ensemble models at x . The QBC criterion quantifies the level of disagreement between the models, and it is assumed to be a good proxy for the level of informativeness of a particular input point, if it were labeled. Due to our focus on deep learning, we assume that the ensemble is composed of DNNs.

The pool ratio hyperparameter. A well-known limitation of QBC, as well as other pool-based AL algorithms, is their dependency on their pool size, N_U [16, 4, 17]. A larger value of N_U can lead to the discovery of points with larger σ_{QBC} because the input space is sampled more densely; however, larger N_U also tends to increase the similarity of the points, so that they provide the same information to the model - a problem sometimes called mode collapse [16, 4, 17]. In the limit as $N_U \rightarrow \infty$ all of the k selected query points will be located in near the same $x \in \chi$ that has the highest value of σ_{QBC} . The negative impact of excessively small and large values of N_U , respectively, is illustrated in Fig. 1(a-b) for a simple 1-dimensional problem and summarized in Fig. 1(d). The step size, k , of the active learning model also interacts strongly with the pool size, and therefore the ratio of pool size to step size is treated as a single

Algorithm 1 Query-by-committee (QBC) Pool-based active learning

Input: Initial small labeled training set T_0 , unlabeled set U , step size k , number of steps S , models f_i

```

for  $s = 1$  to  $S$  do
  for  $n = 1$  to  $N$  do
    Train  $f_n$  using training set  $T$ 
  end for
  for  $x_j \in U$  do
    Calculate  $\sigma^2$ 
  end for
  Sort  $\sigma^2$ , take the top  $k$ 
  Let oracle label the top  $k$  ones, add them into  $T$ 
end for

```

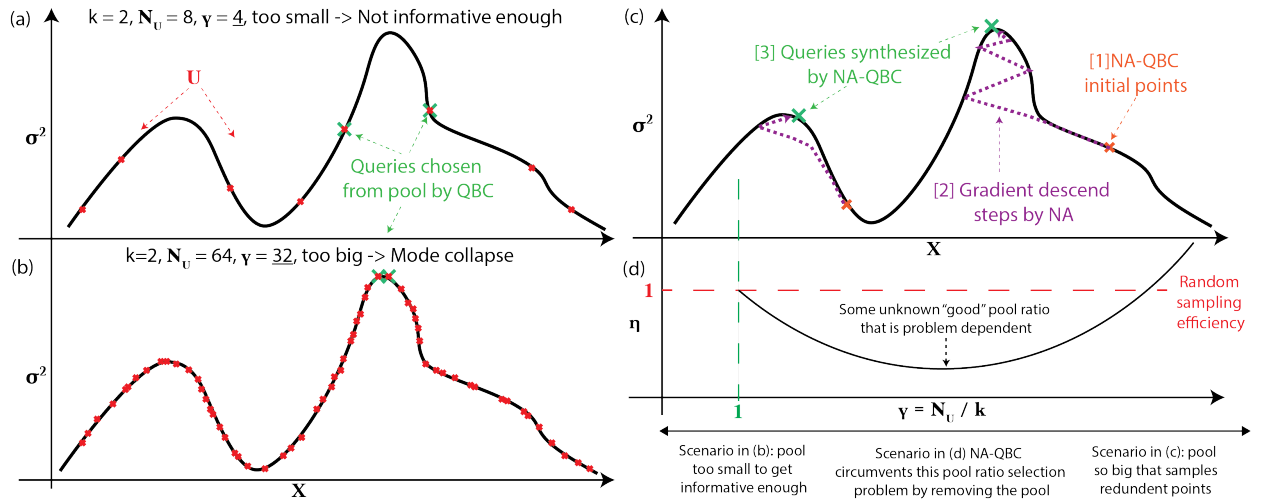


Figure 1: Schematic diagram for QBC and NA-QBC mechanism. (a, b) are two scenarios of the pool ratio (γ) being too small (4 in b) or too large (32 in c) in k (step size) of 2. (c) Working mechanism of NA-QBC. (d) Schematic for η (AL Efficiency) vs pool ratio for QBC method: As either too small or too large of a pool ratio would be harmful to AL efficiency with some unknown good ratio hard to know a priori, NA-QBC circumvents the problem by removing the pool. Note that while pool ratio of 1 makes QBC equivalent to random sampling and smaller values of pool ratio is undefined.

hyperparameter,

$$\gamma = N_U/k. \quad (2)$$

Crucially, and as we show in our experiments, choosing a sub-optimal γ value not only reduces the benefits of QBC, but also can cause it to perform worse than naive random sampling. Typically the optimal value of γ balances

This isn't necessarily a problem if an appropriate value of γ can be chosen, however the optimal value of γ depends heavily upon the particular problem being considered. This is evidenced by the widely-varying values of γ that are utilized in the literature: e.g., 17000 [31], 20 to 2000 [17], 300 to 375 [32], 11-20 [8], 1000 [16], and 1 to 11 [33]. We corroborate these findings with our four benchmark problems in Sec. 6 as well. Furthermore, and to the best of our knowledge, γ also cannot be reliably chosen without first collecting a substantial quantity of *labeled* data. This greatly undermines the value of QBC, and pool-based AL methods in general, since one cannot know in advance whether such methods will achieve better results than simple random sampling.

4 Neural adjoint QBC

The NA-QBC method attempts to *efficiently* search over all $x \in \chi$ to find those that maximize the QBC criterion, which can be framed as the following optimization problem

$$\operatorname{argmax}_{x \in \chi} \sigma_{QBC}^2(x) \quad (3)$$

The solutions to this optimization then are synthesized and labeled. By assumption in Sec. 3, we assume that χ is a well-defined space of admissible solutions and that we have an oracle that can accurately label any $x \in \chi$ (e.g., a mathematical model, or simulator). These are reasonable assumptions for a wide array of problems in science and engineering, including those in our benchmark problems.

To solve this optimization problem we leverage the recently-proposed NA method [34], which can minimize (or, equivalently, maximize) an arbitrary black-box function, $f(x)$ with respect to its input x . A major assumption of NA is that it can accurately approximate f with a DNN, \hat{f} , providing an analytic and differentiable expression relating the output of f to its input x . Therefore it is possible to use the DNN approximation to efficiently minimize \hat{f} with respect to its input x using gradient descent (via backpropagation), starting from some randomly-initialized location within the domain of x . More formally, let \hat{x}^i be our current estimate of the solution, where i indexes each solution we obtain in an iterative gradient-based estimation procedure. Then we compute \hat{x}^{i+1} with

$$\hat{x}^{i+1} = \hat{x}^i - \alpha \left. \frac{\partial \hat{f}(\hat{x}^i)}{\partial x} \right|_{x=\hat{x}^i} \quad (4)$$

where α is the learning rate, which can be made adaptive using conventional approaches like Adam [35]. This optimization procedure only finds a locally optimal solution to Eq. 3, however, the NA approach overcomes this limitation by creating a large number of N_{NA} initializations, and then optimizing each one using Eq. 4. The best solution among each of these N_{NA} candidates can be found by passing them back into the DNN surrogate, \hat{f} .

Lastly, to ensure that the identified solutions remain within the admissible domain of x (also where the DNN surrogate is accurate) the NA method employs a "boundary loss" that encourages solutions to stay within the domain of x . The boundary loss is formally defined in Eq 5:

$$\mathcal{L}_{boundary}(\hat{x}) = ReLU(|\hat{x} - x_{mid}| - 0.5 * R_x) \quad (5)$$

where ReLU is rectified linear unit, x_{mid} is the middle point of the hypercube of our problem domain and R_x is the dimension-wise range.

We can directly apply the NA to solve Eq. 3 by recognizing that the QBC criterion is composed of an ensemble of DNNs, and therefore we can treat $\sigma_{QBC}(x)$ as \hat{f} in the NA. To obtain multiple query synthesis points from the NA method (i.e., when $k > 1$) we set $N_{NA} = k$, so that we obtain exactly k local minima to retain. The parameters of the boundary loss in Eq. 5 can readily be derived from χ , the QBC x -space. The NA method has recently proven to be a state-of-the-art inverse solver for regression problems [36, 34], making it highly effective at finding points that maximize the QBC criterion.

What makes NA-QBC hyperparameter-free? Although NA-QBC has hyperparameters (discussed below), we say that it is "hyperparameter-free" with respect to AL; this is because it no longer has any sensitive hyperparameters that require labeled data on the target task to optimize. In particular, the NA-QBC no longer requires a γ hyperparameter like QBC. Fundamentally, NA-QBC no longer relies upon sampling density to find informative samples. Instead, it employs a maximally-sparse set of samples (equal to the step size, k), which minimizes redundancy within the limits of the required step size. Despite this sparse sampling however the NA is still capable of finding informative points due to its reliance on gradient descent. Using gradient descent it can converge to highly informative query locations even when starting from a poor random sample. This concept is illustrated in Fig. 1(c). Because NA-QBC initializes with random samples (an typical baseline for AL) and then is guaranteed to improve upon the informativeness of these initializations via gradient descent (or at least not make them worse), it is highly likely that NA-QBC will be as effective as random sampling, and often superior. Our four benchmark experiments corroborate this hypothesis.

As mentioned, NA-QBC does introduce some extra hyperparameters that were not present in the original QBC. We list all these new hyperparameters and provide an explanation regarding why they are either insensitive, or otherwise can be set in advance without the need for labeled data on the target AL task. (1) The maximum backpropagating steps for searching for variance local maximums (S_{bp}): This hyperparameter guarantees convergence and can be enlarged during application when convergence is not observed during QS step. (2) The boundary loss ($\mathcal{L}_{boundary}$): This hyperparameter guarantees the validity of the gradient as it prevents queries "wandering" outside the problem definition region. Same

as S_{bp} , the boundary loss can be enlarged during application time when the variance gradient overpowers boundary loss and pushes queries outside the bounded region. Instead of applying a larger boundary loss, one can also simply re-initialize these query proposals¹. (3) Learning rate during query backpropagation steps (δ): This hyperparameter, together with S_{bp} controls the speed at which the query converges to local maximums. Again, it can be tuned by looking at the convergence plot of variance.

Algorithm 2 Neural-adjoint Query-by-committee (NA-QBC) query synthesis active learning

Input: Initial labeled training set T_0 , step size k , number of active learning steps S , models f_i , **number of backpropagation steps S_{bp} , learning rate α**

```

for  $s = 1$  to  $S$  do
  for  $n = 1$  to  $N$  do
    Train  $f_n$  using training set  $T$ 
  end for
  randomly initialize  $k$  points in  $x$  space as  $X_{add}$ 
  for  $x_j \in X_{add}$  do
    for  $s_{bp} = 1$  to  $S_{bp}$  do
      Calculate  $\mathcal{L} = \mathcal{L}_{boundary} - \sigma^2$ 
      Update:  $x_j \leftarrow x_j + \alpha \frac{d\mathcal{L}}{dx_j}$ 
    end for
  end for
  Let oracle label the  $X_{add}$ , add them into  $T$ 
end for

```

5 Experiment setup

Metric: Data Efficiency (η) A popular performance reporting plot in active learning literature is the accuracy/error vs training dataset size/active learning steps [17, 26, 15, 24, 31]. This is effective for image classification tasks as the goal is majorly higher precision using the same amount of data (as their experiments usually have the same number of total data points). However, for regression-based scientific computing active learning tasks, the focus is usually on how much labeling effort can be saved given the model achieve a target error/accuracy. Instead of showing error vs training dataset curves (which are included in the appendix), we present our results in data efficiency plots, where the x-axis would be the target error (\hat{err}), measured in Mean Squared Error (MSE), and the y-axis would be "data efficiency" calculated by the size of training set needed to reach certain error ($|T_{AL}|(err)$):

$$|T_{AL}(err)| = \min(|T_{AL}|) \text{ s.t. } MSE(\bar{f}_{T_{AL}}) \leq err \quad (6)$$

where $\bar{f}_{T_{AL}}$ is (ensemble) model trained using training set T_{AL} , compared to the size of training set random sampling needs ($|T_{random}(err)|$), where each algorithm is ran 10 times (100 pairs of trails in total and therefore 100 values of η for each AL method as a result), showed in Equation 7.

$$\eta_{AL}(err) = |T_{AL}(err)| / |T_{random}(err)| \quad (7)$$

A data efficiency above one signifies the active learning method is harmful to such error level as more data points need to be sampled on average compared to random sampling.

Experiment outline and cross-dataset generalization measurement η_{real} We run both QBC and NA-QBC on each of our benchmark datasets from a small initial labeled training set. We stop each of the algorithms by setting a fixed mean squared error threshold on a pre-defined, large test set on each of our datasets (all AL models keep collecting more data points until reaching some predefined error target (\hat{err}) threshold). To prevent random fluctuation dominating our observation, we require the test MSE to be less than or equal to the \hat{err} for 5 occurrences for both stopping criteria and $|T|$ calculations. For each of the datasets, an appropriate architecture of the neural network is assumed to be known a priori and we get the architecture by tuning hyperparameters on a large labeled dataset or from previously reported benchmarks (two materials datasets). We vary γ in the range from 2 to 256 with a multiplication rate of 2. Every experiment is conducted 10 times and we report the mean and 25th/75th percentile for reference of the fluctuations.

To further test the real-world performance of QBC after taking the hyperparameter into account, we propose to sample the pool ratio γ from the real-world distribution. As the four datasets already represent our belief of real-world scenarios,

¹In our experiment, we did find there are occasionally (1%) queries outside our defined boundary although a relatively large boundary loss is applied and we adopt this method.

we propose to use one dataset as "known" dataset (A) where optimal pool ratio (γ_A) is known or found by optimization and test QBC's performance on another dataset (B) using this optimal ratio value.

$$\eta_{real}|_B = \eta_{\gamma_A}|_B \text{ s.t. } \gamma_A = \underset{\gamma=|N_U|/k}{\operatorname{argmin}} \eta_\gamma|_A \quad (8)$$

where $|_B$ represent evaluated on dataset B and η_r represent the QBC efficiency at $e\hat{r}$ specified in table 1. For η_{real} for NA-QBC, as it does not have hyperparameter of r , its η_{real} is its measured efficiency at each dataset. Since this measure is dependent on both known dataset A and test dataset B, we calculate η_{real} for all 12 pairs and report whether QBC's η_{real} is better than η_{NA} in all 12 cases.

Table 1: Set up for our benchmark experiments. $Dim_{x,y}$ are the dimensionality of x and y. The target error ($e\hat{r}$, the stopping criteria) is chosen trading off between applicability and computation time. Number of committee (# COM) is fixed at 10 except for ADM problem where GPU RAM limits it to 5. For the architecture, they are represented in axb format where a is the number of neurons per hidden layer and b is the number of hidden layers (excluding input and output layer). Arch represent the network architecture (*: for ADM, there are 3 layers of convolutions after the linear layer)

FEATURES	SINE	ROBO	STACK	ADM
Dim_x	1	4	5	14
Dim_y	1	2	201	2000
$e\hat{r}$	1E-3	5E-5	3E-5	3E-3
# COM	10	10	10	5
N_{ini}	80	50	50	300
$ k $	40	50	50	50
$ D_{test} $	4000	4000	4000	4000
ARCH	20×9	500×4	700×9	$1500 \times 6^*$

Benchmark Datasets In order to compare our active learning method with QBC in diverse settings, four datasets have been selected. Note that usually public datasets, like the UCI dataset, would not work due to QS needing the oracle forward model to be evaluated. Among the four datasets benchmarked, two are toy datasets and two are real scientific computing regression tasks (from material science) that are repurposed into active learning benchmarking.

1D sine wave dataset. We start with an 1D input 1D output toy problem that is composed of sinusoidal waves.

$$y = x * \sin(a_1 * \sin(a_2 * x))$$

where $a_1 = 3$ and $a_2 = 30$ is chosen to make a relative complicated loss surface for the neural network to learn while also having a difference in sensitivity in the domain of x.

2D robotic arm dataset. For the second benchmark dataset, We adapted the historic robotic arm problem from [24].

$$y_0 = \sum_{i=1}^3 \cos(\frac{pi}{2} x_i) * l_i, y_1 = x_0 + \sum_{i=1}^3 \sin(\frac{pi}{2} x_i) * l_i$$

where y is the position in the 2D plane, x_0 is the adjustable starting horizontal position, $x_{i=1,2,3}$ are the angles of the arm relative to horizontal reference and $l_{i=1,2,3} = [0.5, 0.5, 1]$ represents the i-th length of the robotic arm component.

Stacked layered materials (Stack). A simple material design dataset that has analytical solution coded mapping from geometry space, a series of stacks, to response space, the reflection spectra of the absorber as a function of wavelength (illustration in Appendix). First published in [37], it became one of the benchmark problems in [38].

Artificial Dielectric Material (ADM). ADM dataset is a repurposed high dimensional physics scientific computing example in material design published in recent benchmark for scientific computing for emulators [39]. This dataset consists of input space of 3D geometric shape parameterized into 14 dimension space and the output is the spectral response of the material.

All our datasets are generated with a range of the hypercube of $x \in [-1, 1]$.

6 Result

The main experimental results are presented in Fig 2. The left column is the data efficiency η plot and the right column is the efficiency at the target MSE value (the right-most point of the left plots). As the error usually decreases

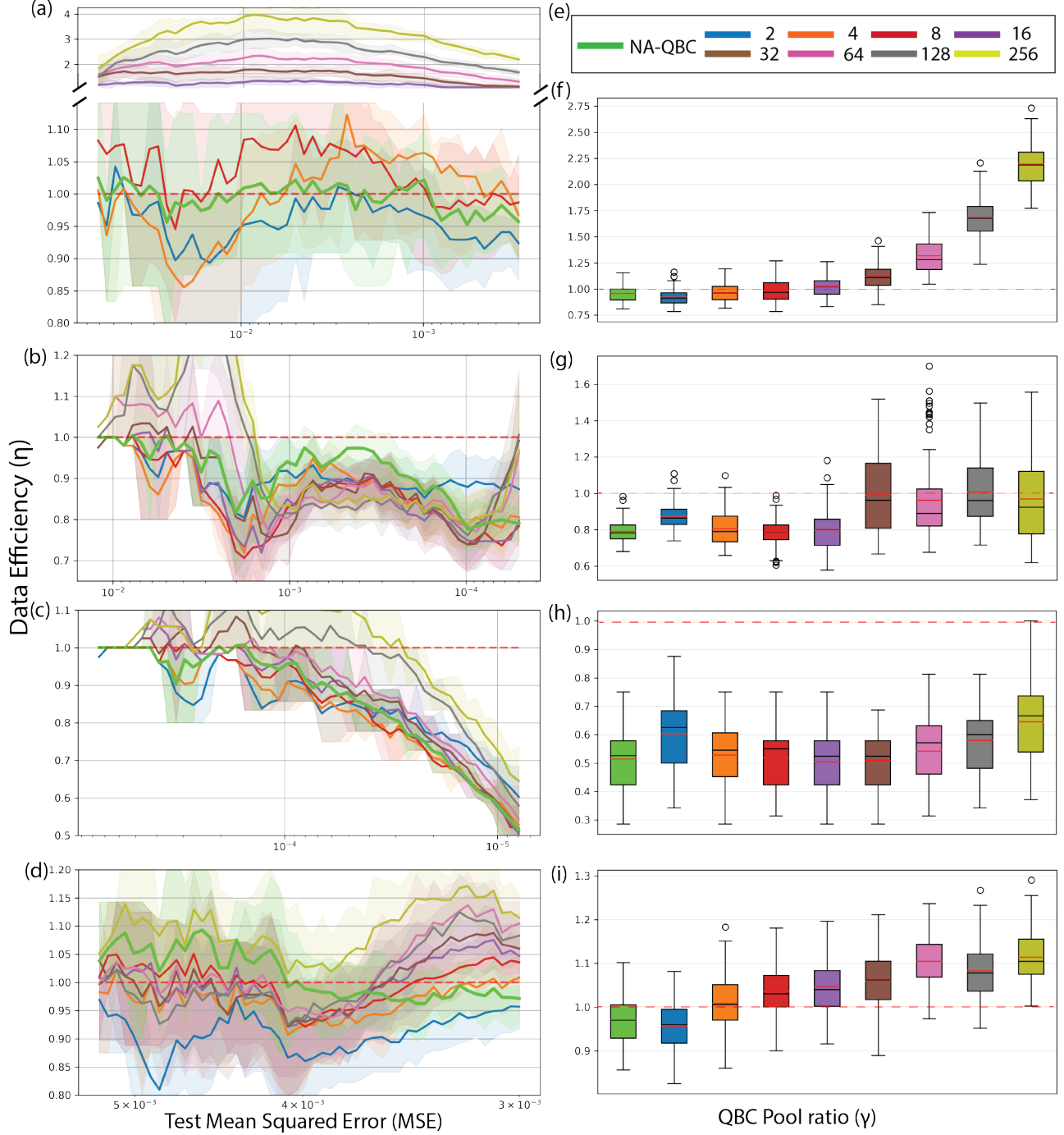


Figure 2: Performance plot comparing QBC and NA-QBC, both relative to random sampling. (a-d) are data efficiency η vs test MSE plot where x-axis is the test MSE. The legend for colors are presented at (e) where the numbers represent the pool ratio γ for QBCs used (for example: ratio of 2 means QBC would choose k points out of a pool of $2k$ unlabeled points). (f-i) are box plots of the data efficiency at e_{rr} (rightmost MSE at the left column) for each datasets. In the box, black line represent the median and red line represent mean values. (a,f): Sine wave dataset. (b,g): Robotic arm dataset. (c,h): Stack dataset. (d, i): ADM dataset. The red dashed line of random sampling efficiency is added for reference. The y axis of all plots are data efficiency η compared to random sampling defined in eq 7

exponentially with the increase of dataset size, the "important" η that determines the effectiveness of AL algorithms would be closer to the right side (where the error is much smaller and error reduces much slower). Here we take the final target MSE \hat{err} to emphasize using the right columns. Notably in Fig 2(a-d), η varies widely with different pool ratio γ being selected. For example, for sine wave dataset (Fig 2a and f), although a γ of 2 can reliably get a performance boost by choosing active learning instead of random sampling, a poorly chosen γ (such as 32, 64, 128 and 256) can be catastrophic to the data collection process as it suffers from the mode collapsing illustrated in Fig 1.

On the contrary of QBC's sensitive behavior w.r.t. pool ratio γ , NA-QBC performs much more robust than QBC. Among the 8 γ choices, judging by median efficiency across 10 trials, NA-QBC always ranks in top 3 with a marginal difference with the best-performing one (if it is not the top-performing one). More importantly, while the optimal γ is dependent on the structure of the problem (hence hard to know in advance before having labeled data), NA-QBC's stability in performance is highly desired in the application stage where active learning is applied to a new problem without knowing the possible working pool ratio range.

To further show the performance of NA-QBC and QBC in real scenarios, comparison using real efficiency (η_{real} defined in Eq 8) are shown in Table 2. From the table, we can see that out of 12 pair-wise trails, NA-QBC outperforms QBC 8 out of 12 times (p value < 0.05) and performs comparably 3 out of 12 times. Only in the robotic arm \rightarrow ADM pair does QBC (1 out of 12 times) win in data efficiency, which further assures the robustness of NA-QBC compared to QBC. One might argue that during real-life applications, one would choose the hyperparameter from similar problems. If datasets are separated by toy/material criteria, NA wins in all four pairs (Sine \leftrightarrow Robo, Stack \leftrightarrow ADM) of similar problems.

Table 2: Real world performance η_{real} comparison between QBC and NA-QBC. As defined in Eq 8, the pool ratio γ is chosen from the mean efficiency at the \hat{err} of each dataset and is labeled in [] after the dataset. For each train/test pair, we label whether NA or QBC win the comparison by independent t-test without the assumption of same population variance. The winning criteria is p-value (which is labeled in () after each results) lower than 0.05. For race where p-value is larger than 0.05, we label them as draw as there is not enough evidence that their mean is different from the samples drawn.

γ SELECTED FROM \downarrow TEST ON \rightarrow	SINE-WAVE	ROBOTIC ARM	STACK	ADM
SINE-WAVE [2]	-	NA(1E-16)	NA(1E-7)	DRAW(0.06)
ROBOTIC ARM [8]	NA(0.03)	-	DRAW (0.75)	NA (1E-14)
STACK [16]	NA(2E-7)	DRAW (0.60)	-	NA(1E-17)
ADM [2]	QBC(3E-3)	NA(2E-16)	NA(1E-7)	-

7 Conclusion

In this work, we present the hyperparameter selection issue faced by the popular active learning QBC method in four benchmark regression problems. We find that the highly sensitive pool ratio γ makes QBC much limited in application to new regression problems and, by considering the query selection process as an inverse problem and combining QBC with inverse solver Neural Adjoint, we innovate NA-QBC as the first query synthesis deep active learning algorithm that is robust as it does not depend on any pool to select queries for next step, making it an effectively zero hyperparameter version of QBC approach. We also propose a data efficiency metric η that better captures the effect of active learning in scientific computing scenarios and shows NA-QBC's robustness on different problems using this metric. Finally, we test QBC and our zero hyperparameter version NA-QBC on real-world performance with cross-dataset generalization metric η_{real} where γ is optimized in a known dataset and tested on a new dataset. The cross-dataset experiments show NA-QBC dominates QBC when considering the hyperparameter selection process.

References

- [1] J. Jumper, R. Evans, A. Pritzel, T. Green, M. Figurnov, O. Ronneberger, K. Tunyasuvunakool, R. Bates, A. Žídek, A. Potapenko, *et al.*, "Highly accurate protein structure prediction with alphafold," *Nature*, vol. 596, no. 7873, pp. 583–589, 2021.
- [2] D. Rolnick, P. L. Donti, L. H. Kaack, K. Kochanski, A. Lacoste, K. Sankaran, A. S. Ross, N. Milojevic-Dupont, N. Jaques, A. Waldman-Brown, *et al.*, "Tackling climate change with machine learning," *arXiv preprint arXiv:1906.05433*, 2019.

- [3] A. Lavin, H. Zenil, B. Paige, D. Krakauer, J. Gottschlich, T. Mattson, A. Anandkumar, S. Choudry, K. Rocki, A. G. Baydin, *et al.*, “Simulation intelligence: Towards a new generation of scientific methods,” *arXiv preprint arXiv:2112.03235*, 2021.
- [4] P. Ren, Y. Xiao, X. Chang, P.-Y. Huang, Z. Li, B. B. Gupta, X. Chen, and X. Wang, “A survey of deep active learning,” *ACM Computing Surveys (CSUR)*, vol. 54, no. 9, pp. 1–40, 2021.
- [5] B. Settles, “Active learning literature survey,” 2009.
- [6] P. Kumar and A. Gupta, “Active learning query strategies for classification, regression, and clustering: a survey,” *Journal of Computer Science and Technology*, vol. 35, no. 4, pp. 913–945, 2020.
- [7] H. S. Seung, M. Oppor, and H. Sompolinsky, “Query by committee,” in *Proceedings of the fifth annual workshop on Computational learning theory*, pp. 287–294, 1992.
- [8] S. Roy, A. Unmesh, and V. P. Namboodiri, “Deep active learning for object detection.,” in *BMVC*, vol. 362, p. 91, 2018.
- [9] J.-J. Zhu and J. Bento, “Generative adversarial active learning,” *arXiv preprint arXiv:1702.07956*, 2017.
- [10] D. Mahapatra, B. Bozorgtabar, J.-P. Thiran, and M. Reyes, “Efficient active learning for image classification and segmentation using a sample selection and conditional generative adversarial network,” in *International Conference on Medical Image Computing and Computer-Assisted Intervention*, pp. 580–588, Springer, 2018.
- [11] A. Englhardt and K. Böhm, “Exploring the unknown—query synthesis in one-class active learning,” in *Proceedings of the 2020 SIAM International Conference on Data Mining*, pp. 145–153, SIAM, 2020.
- [12] K. T. Schütt, M. Gastegger, A. Tkatchenko, K.-R. Müller, and R. J. Maurer, “Unifying machine learning and quantum chemistry with a deep neural network for molecular wavefunctions,” *Nature communications*, vol. 10, no. 1, pp. 1–10, 2019.
- [13] C. C. Nadell, B. Huang, J. M. Malof, and W. J. Padilla, “Deep learning for accelerated all-dielectric metasurface design,” *Optics express*, vol. 27, no. 20, pp. 27523–27535, 2019.
- [14] A. Zhavoronkov, Y. A. Ivanenkov, A. Aliper, M. S. Veselov, V. A. Aladinskiy, A. V. Aladinskaya, V. A. Terentiev, D. A. Polykovskiy, M. D. Kuznetsov, A. Asadulaev, *et al.*, “Deep learning enables rapid identification of potent ddr1 kinase inhibitors,” *Nature biotechnology*, vol. 37, no. 9, pp. 1038–1040, 2019.
- [15] E. Tsymbalov, M. Panov, and A. Shapeev, “Dropout-based active learning for regression,” in *International conference on analysis of images, social networks and texts*, pp. 247–258, Springer, 2018.
- [16] R. Burbidge, J. J. Rowland, and R. D. King, “Active learning for regression based on query by committee,” in *International conference on intelligent data engineering and automated learning*, pp. 209–218, Springer, 2007.
- [17] S. Kee, E. Del Castillo, and G. Runger, “Query-by-committee improvement with diversity and density in batch active learning,” *Information Sciences*, vol. 454, pp. 401–418, 2018.
- [18] D. Angluin, “Queries and concept learning,” *Machine learning*, vol. 2, no. 4, pp. 319–342, 1988.
- [19] E. B. Baum and K. Lang, “Query learning can work poorly when a human oracle is used,” in *International joint conference on neural networks*, vol. 8, p. 8, 1992.
- [20] E. B. Baum, “Neural net algorithms that learn in polynomial time from examples and queries,” *IEEE Transactions on Neural Networks*, vol. 2, no. 1, pp. 5–19, 1991.
- [21] L. Wang, X. Hu, B. Yuan, and J. Lu, “Active learning via query synthesis and nearest neighbour search,” *Neurocomputing*, vol. 147, pp. 426–434, 2015.
- [22] R. D. King, K. E. Whelan, F. M. Jones, P. G. Reiser, C. H. Bryant, S. H. Muggleton, D. B. Kell, and S. G. Oliver, “Functional genomic hypothesis generation and experimentation by a robot scientist,” *Nature*, vol. 427, no. 6971, pp. 247–252, 2004.
- [23] R. D. King, J. Rowland, S. G. Oliver, M. Young, W. Aubrey, E. Byrne, M. Liakata, M. Markham, P. Pir, L. N. Soldatova, *et al.*, “The automation of science,” *Science*, vol. 324, no. 5923, pp. 85–89, 2009.
- [24] D. A. Cohn, Z. Ghahramani, and M. I. Jordan, “Active learning with statistical models,” *Journal of artificial intelligence research*, vol. 4, pp. 129–145, 1996.
- [25] C. Mayer and R. Timofte, “Adversarial sampling for active learning,” in *Proceedings of the IEEE/CVF Winter Conference on Applications of Computer Vision*, pp. 3071–3079, 2020.
- [26] I. Guyon, G. C. Cawley, G. Dror, and V. Lemaire, “Results of the active learning challenge,” in *Active Learning and Experimental Design workshop In conjunction with AISTATS 2010*, pp. 19–45, JMLR Workshop and Conference Proceedings, 2011.

- [27] B. Settles, *Curious machines: Active learning with structured instances*. PhD thesis, University of Wisconsin–Madison, 2008.
- [28] W. Cai, Y. Zhang, and J. Zhou, “Maximizing expected model change for active learning in regression,” in *2013 IEEE 13th international conference on data mining*, pp. 51–60, IEEE, 2013.
- [29] C. Käding, E. Rodner, A. Freytag, O. Mothes, B. Barz, J. Denzler, and C. Z. AG, “Active learning for regression tasks with expected model output changes,” in *BMVC*, p. 103, 2018.
- [30] J. S. Smith, B. Nebgen, N. Lubbers, O. Isayev, and A. E. Roitberg, “Less is more: Sampling chemical space with active learning,” *The Journal of chemical physics*, vol. 148, no. 24, p. 241733, 2018.
- [31] A. K. McCallumzy and K. Nigamy, “Employing em and pool-based active learning for text classification,” in *Proc. International Conference on Machine Learning (ICML)*, pp. 359–367, Citeseer, 1998.
- [32] J. E. Santos, M. Mehana, H. Wu, M. Prodanovic, Q. Kang, N. Lubbers, H. Viswanathan, and M. J. Pyrcz, “Modeling nanoconfinement effects using active learning,” *The Journal of Physical Chemistry C*, vol. 124, no. 40, pp. 22200–22211, 2020.
- [33] Y. Tan, L. Yang, Q. Hu, and Z. Du, “Batch mode active learning for semantic segmentation based on multi-clue sample selection,” in *Proceedings of the 28th ACM International Conference on Information and Knowledge Management*, pp. 831–840, 2019.
- [34] S. Ren, W. Padilla, and J. Malof, “Benchmarking deep inverse models over time, and the neural-adjoint method,” *arXiv preprint arXiv:2009.12919*, 2020.
- [35] D. P. Kingma and J. Ba, “Adam: A method for stochastic optimization,” *arXiv preprint arXiv:1412.6980*, 2014.
- [36] Y. Deng, S. Ren, K. Fan, J. M. Malof, and W. J. Padilla, “Neural-adjoint method for the inverse design of all-dielectric metasurfaces,” *Optics Express*, vol. 29, no. 5, pp. 7526–7534, 2021.
- [37] Y. Chen, J. Zhu, Y. Xie, N. Feng, and Q. H. Liu, “Smart inverse design of graphene-based photonic metamaterials by an adaptive artificial neural network,” *Nanoscale*, vol. 11, no. 19, pp. 9749–9755, 2019.
- [38] S. Ren, A. Mahendra, O. Khatib, Y. Deng, W. J. Padilla, and J. M. Malof, “Inverse deep learning methods and benchmarks for artificial electromagnetic material design,” *arXiv preprint arXiv:2112.10254*, 2021.
- [39] Y. Deng, J. Dong, S. Ren, O. Khatib, M. Soltani, V. Tarokh, W. Padilla, and J. Malof, “Benchmarking data-driven surrogate simulators for artificial electromagnetic materials,” in *Thirty-fifth Conference on Neural Information Processing Systems Datasets and Benchmarks Track (Round 2)*, 2021.

A Error vs training data size plots

To supplement our discussion in the main text, although we used the metric of data efficiency, below Fig 3 shows the MSE vs training set size. Note that for plotting this, a smoothing parameter of 0.3 is applied using Tensorboard visualization smoothing function. Also the curves are plotted to the smallest training set size of each hyper-parameter choice. (As a MSE threshold is set as stopping criteria, the number of active learning step varies even within the same hyperparameter due to random fluctuations.) The shaded area is the standard deviation (std) with upper bound being mean + std and lower bound being mean - std.

B Dataset illustrations

Here we present the illustration for our benchmark datasets used. Fig 4 shows the schematic diagram of the sine wave and robotic arm datasets. Fig 5 shows the schematic diagram of the the meta-material design Stack and ADM datasets.

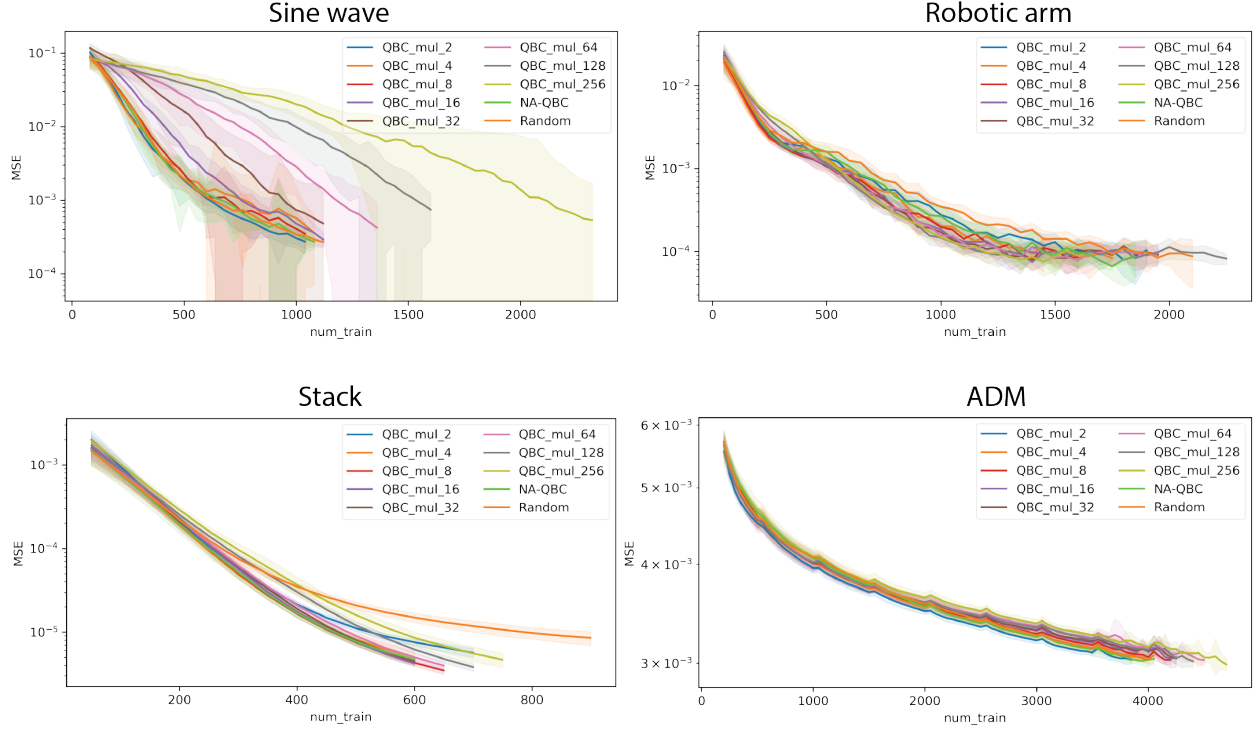


Figure 3: Traditional error vs training set size plot for all datasets

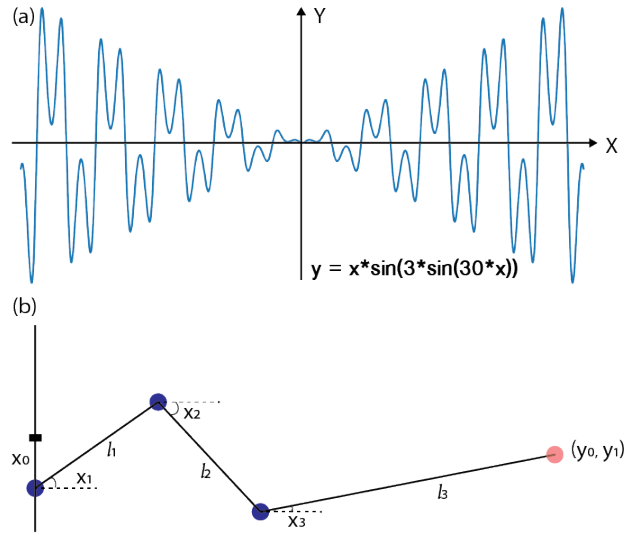


Figure 4: Schematic illustration of sine wave and robotic arm datasets

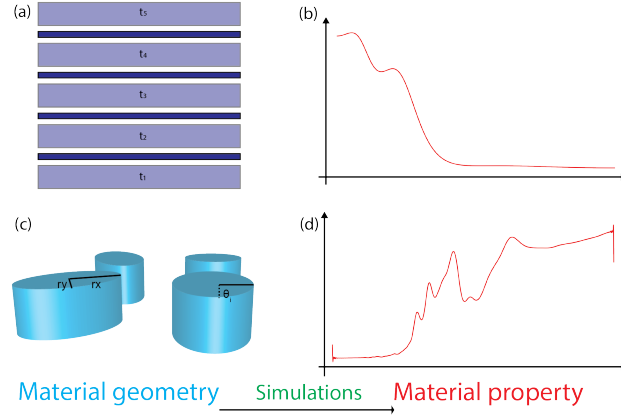


Figure 5: (a, c) are schematic illustration of two material design datasets (Stack & ADM). (b, d) are example spectra of their material property after simulations from their geometric parameterization (typically from Maxwell equation solvers that are slow and hence can benefit from active learning)